J MATER SCI **41** (2006) 1623–1630

X-ray and ion emission characteristics of plasmas ablated from solid materials using a high power Nd:Glass laser

L. J. DHARESHWAR*, S. CHAURASIA, C. G. MURALI, N. K. GUPTA, B. K. GODWAL
High Pressure Physics Division, Bhabha Atomic Research Centre, Trombay, Mumbai 400085, India
E-mail: dharesh@apsara.barc.ernet.in

X-ray and ion emissions from high temperature plasmas from solid targets with different atomic numbers have been studied. Plasma is generated using a high power Nd:Glass laser generating focused intensity in the range of 10^{12} to 10^{13} Watts/cm^2 on targets. Plasma temperature is typically between 50 to 100 eV. X-ray emission scaling as a function of laser intensity as well as ion velocity has been measured in these targets. Non-uniform plasma expansion and generation of fast ions are observed for targets with higher atomic numbers.

1. Introduction

High power lasers when focused on materials can produce plasmas at extremely high temperature and ablate material at a very high rate. Simultaneously, a very high pressure shock wave propagates in the material creating highly compressed and heated matter. These states of matter, generated on laboratory scale, are of great interest in material science. Interesting results have been reported on studies on shock compressed iron above 3 Mbars using high power lasers. Iron being a major component of earth's core, its Equation of State (EOS) determination has implications in the description of various thermodynamic properties of the core. The very first experiments on Iron between 1 to 10 Megabars were performed by Koenig *et al* [1]. Inertial Confinement Fusion studies with large, Kilojoule class of lasers have been able to generate pressure of 750 Megabars and material compression up to a hundred times the solid density [2]. Elements from Hydrogen to Uranium have been extensively studied while subjected to extreme pressure and temperature using ultra-high power lasers.

Laser produced plasmas are dense, at high temperature and are short lived, having life time of picoseconds to nanoseconds and also intense sources of X-rays and ions. These emissions can be used as probes in the time resolved studies of materials subjected to ultra-high pressure and temperature. Emission of X-rays and ions from dense, high temperature plasmas are therefore an important area of investigation. Lifetime of this laser-plasma X-ray source strongly depends upon the laser pulse duration and the brightness of the X-ray source depends on the laser intensity. Hence, it is essential to determine X-ray emission scaling with laser intensity as well as ion emission characteristics in different target materials. These table top laser based X-ray sources are an attractive alternative and compete with the synchrotron source [3]. Such intense X-ray sources have found wide applications in lithography and are extremely useful for investigation of materials on time scales of femtoseconds to picoseconds.

There are several advantages of using high power lasers for studies in material science. Important laser parameters such as-laser intensity, laser pulse duration and wavelength are changeable, thus offering us an opportunity to investigate matter at varying temperature and pressure in different time regimes. The pressure and temperature of materials irradiated with lasers, scale with the laser intensity and wavelength and the scaling laws have been well established [4, 5]. An additional advantage is that, in order to investigate materials at high pressure and temperature, a well synchronized, external optical probe beam can also be generated from the main laser pulse itself. Irradiation spot diameter on the target can also be very easily changed from few micrometers to a millimeter. Laser driven shock waves have been used by Wark *et al* to extensively

*Author to whom all correspondence should be addressed.
0022-2461
DOI: 10.1007/s10853-006-4658-4

investigate the response of crystals in the pressure range of a few tens of Kilobars [6]. Lasers have thus given a remarkable impetus to time resolved studies on dynamic behavior of materials subjected to shocks generated from intense lasers.

We have reported several experimental results on laser plasmas and laser driven shocks in the range of 0.5 to 5 Megabars in various materials with low to high atomic number using a 4 GWatt / 5 nsec Nd:Glass laser [7–10]. We have also established the scaling of ablation pressure with laser intensity in the range of 10^{12} to 5×10^{13} watts / cm^2. A 10 Gigawatt laser system with a 100psec pulse duration and high peak to background contrast ratio is being used in most of the recent experiments [11, 12] in our laboratory.

The work presented in this paper involves a brief description of our efforts in the area of high power Nd:Glass laser systems development for laser-plasma generation followed by diagnostic and measurement techniques for X-rays and ions emitted from laser plasmas. Scaling of X-ray emission with laser intensity, measurement of ion expansion velocity, ablation uniformity and correlation of X-ray emission with ion emission in low Z and high Z targets are the topics presented in this article.

2. Experimental

2.1. Laser systems and plasma diagnostics

The laser system used in these experiments is a 10 Gigawatt peak power laser having a 100 picosecond (subnanosecond) pulse duration and energy per pulse is 1 to 2 Joules [13]. This laser generates laser intensity in the range of 10^{11} to 10^{13} Watt/cm^2 over a spot diameter of 100 to 200 μm on the target surface. Materials in this laser intensity range evaporate and plasma is formed in the early stage of the laser pulse. Ablation pressure has been observed to vary from 50 Kilobars to 10 Megabars in the laser intensity range used. Temperature of the plasma can reach 10^4 to 10^{60} K. Some of our earlier results on plasma ablation using a 4 Gigawatt peak power laser with a 5 nsec pulse duration and pulse energy variable from 2 to 20 Joules, have also been presented in this article for the sake of comparison [14] of plasma hydrodynamics in the two time regimes.

The optical schematic lay out of the high power 100 picosecond laser system used in these experiments is shown in Fig. 1. The inset in the figure shows the spatial and temporal profile of the laser pulse. Duration of this pulse was measured using a commercial optical streak camera as well as a home built scanning second harmonic autocorrelator [15]. The laser was focused using a 100 mm diameter, 50 mm focal length lens on a target material placed within a laser-plasma interaction vacuum chamber evacuated to a pressure- 10^{-6} Torr. Several on-line diagnostics monitor the laser pulse energy, duration, spatial profile etc during every laser shot. Laser intensity profile was almost Gaussian for tight focusing condition with a 30 μm diameter focal spot on target. A more flat profile, up to 500 μm diameter could be obtained by placing the target in the near field of the focusing lens.

Several plasma diagnostics have been set up to measure plasma density, plasma temperature, plasma ablation velocity, ablation pressure, laser driven shock velocity in the target, particle velocity and X-ray emission from targets. Details of all these diagnostics have been described in references [16-19]. Optical shadowgraphy and interferometry diagnostics have been extensively used to study ablation pressure, scaling of pressure with laser

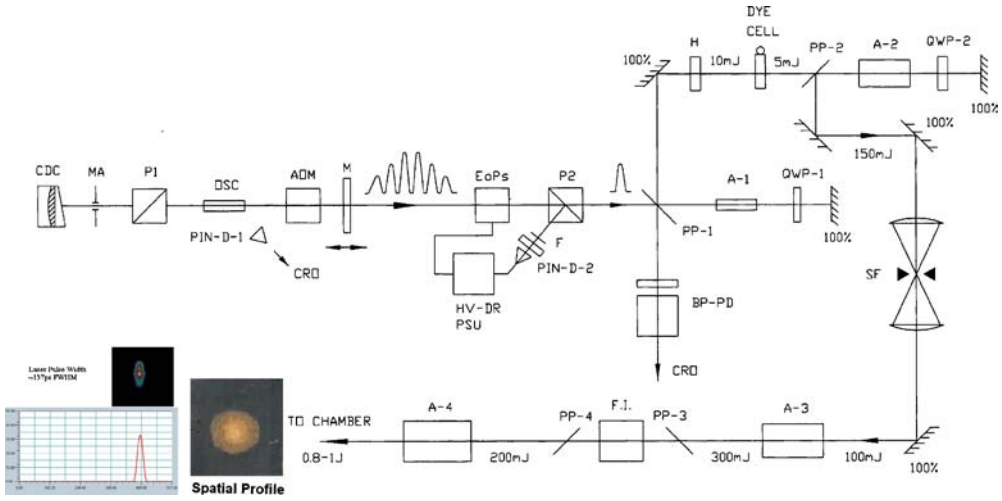

Figure 1 Schematic set up of the 10 GW/100 psec Nd:Glass laser system. CDC–Contacted dye cell of the master oscillator, MA–Mode selecting aperture, P1, P2–glan polarizers, OSC–oscillator active medium, PIN-D-1, PIN-D-2–PIN diode laser detector, M–mirror, EOPS–Electro optic pulse selector, PP-1, PP-2, PP-3–plate polarizers, A-1, 2, 3, 4–Laser Amplifiers, QWP–quarter wave plates, SF–spatial filter, BP-PD–Biplanar photo detector, FI–Faraday Isolator.

intensity, ablating plasma density profiles in targets of varying atomic numbers and density scale lengths using the nanosecond laser system. Shock pressure was measured to be in the range 0.5 to 5 Megabars and plasma electron density varied from 10^{18} to $10^{19} cc^{-1}$. X-ray diagnostics used in the present experiments reported in this paper include- X-ray pin-hole camera with a 25 μm spatial resolution and 5X magnification to obtain the spatial extent of the laser plasma and uniformity of the expanding plasma and X-ray Pin diodes to measure X-ray emission and its scaling with laser intensity from solid copper targets. Time of flight technique has been used with a Langmuir probe to obtain velocity of the ions generated from the ablating material.

2.2. Experiments on laser plasma

2.2.1. X-Ray emission from laser produced plasma from copper targets

Measurement of X-ray emission from a laser irradiated solid copper target and its scaling with laser intensity has been determined in the laser intensity range 10^{12} to 10^{13} W/cm^2. X-ray diode diagnostic head was placed within the laser-plasma interaction vacuum chamber at a distance of 150 mm from the target at 45^0 with respect to the target normal as shown in the experimental scheme of Fig. 2.

The X-ray diodes were covered with suitable X-ray filter foils to record the X-ray emission in different ranges of wavelength. In order to have a broad spectral range of operation, X-ray pin diodes were covered with the filters suitable for the soft as well as the hard part of the considered spectrum. The diagnostic head mounted on a vacuum flange is shown in Fig. 3a.

The X-ray detectors were reverse biased at 300 V as shown in Fig. 3b and were found to have a linear response

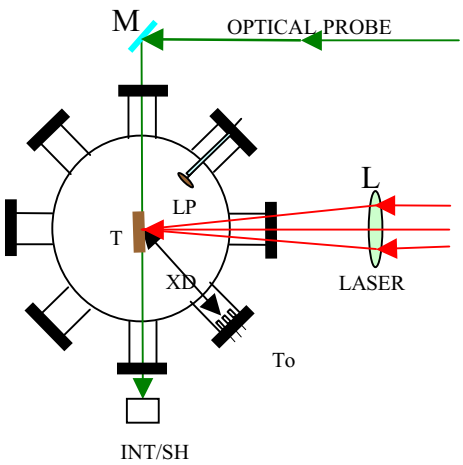

Figure 2 Plasma diagnostic set up in the laser–plasma interaction chamber, L–Laser focusing lens, LP–Langmuir probe, XD–X-ray diodes, T– target, M–mirror, INT/SHAD–Interferogram/ shadowgram recording camera.

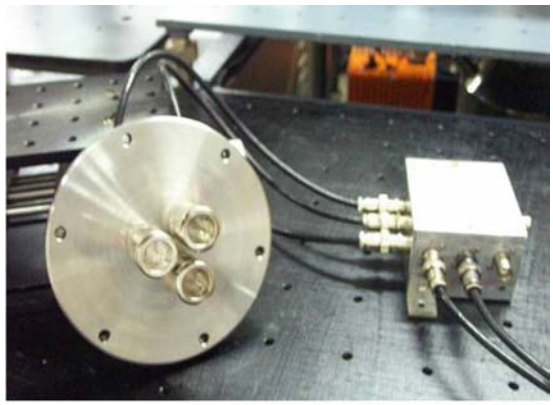

(a)

Figure 3a Photograph of X-ray PIN diode set up.

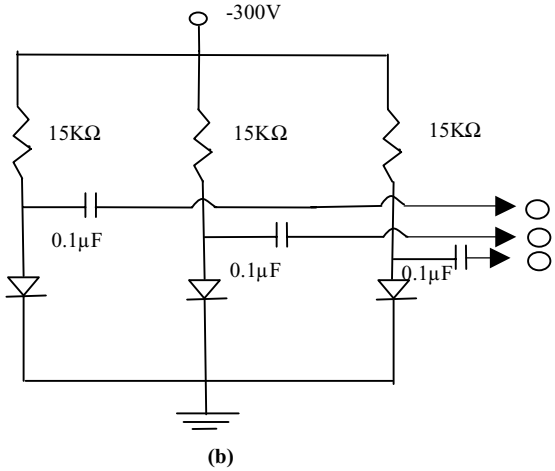

(b)

Figure 3b Biasing circuit for the detectors.

up to a signal level of 100 V.These double diffused silicon pin diodes have an active area of 100 mm^2, depletion depth of 250 μm and rise time of 5 ns.

Since the response of the detectors is slow compared to the sub-nanosecond laser pulse duration, this set up records the integrated X-ray emission during the laser pulse.

The X-ray filter foils were- 12 μm thick Titanium foil having an X-ray absorption K-edge at 4.96 KeV and a 5 μm thick Nickel foil with its K-edge at 8.32 KeV. The transmission curves for the filter foils is shown in Fig. 4a.The typical signals generated by the two X-ray pin diodes and displayed on a 500 MHz storage oscilloscope are shown in Fig. 4b. Peak of the X-ray signal is taken into consideration for record. Laser pulse energy was varied from 250 to 450mJ, thus varying the intensity from 3×10^{12} to 7×10^{12} watts/cm^2. X-ray emission variation in copper plasma with laser intensity for the two different X-ray filters is shown in Fig. 5.

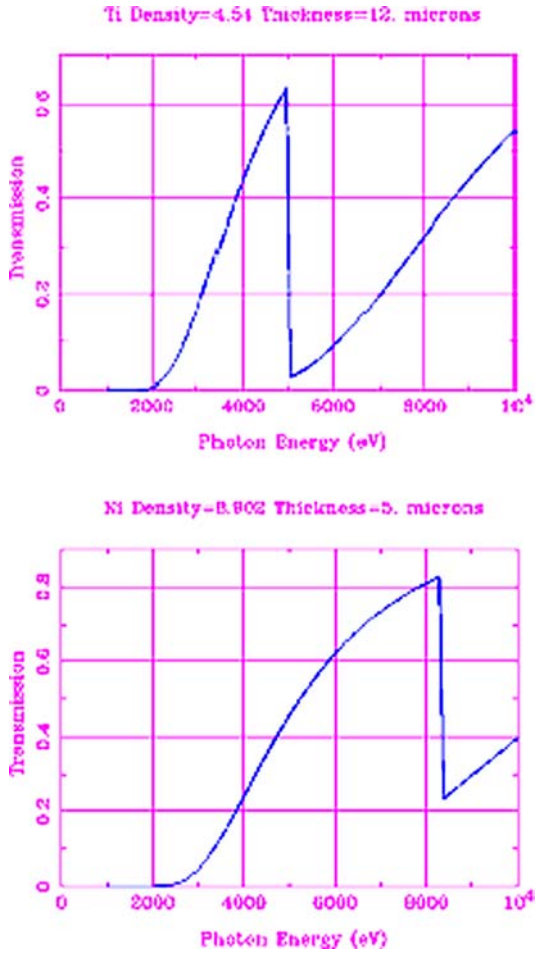

Figure 4a Transmission of X-ray filter foils.

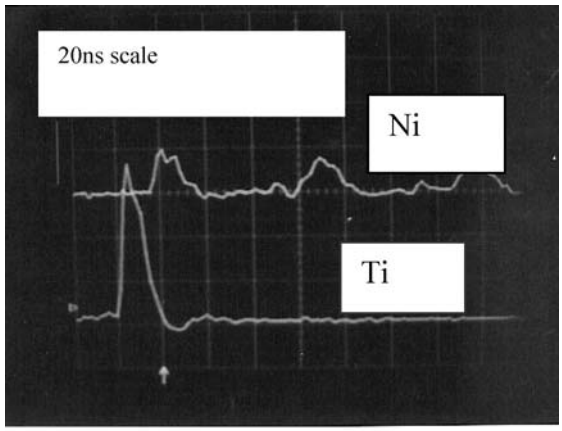

(b)

Figure 4b X-ray emission signals from plasma displayed on oscilloscope.

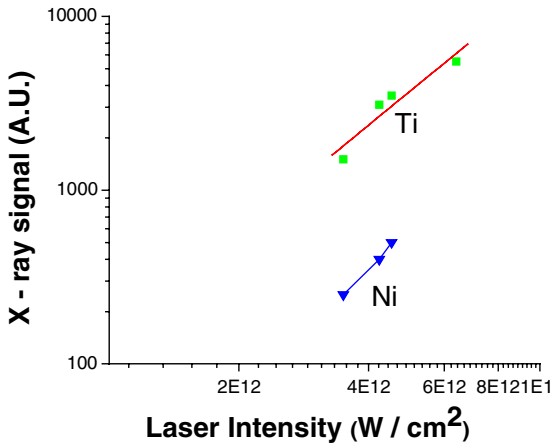

Figure 5 X-ray signal height (in arbitrary units) as a function of laser intensity.

2.2.2. *Measurement of material ablation and ion emission for targets with varying atomic numbers*

Characteristics of material ablation from lower atomic number (Magnesium) to higher atomic number (gold) targets have been compared for plasmas generated by the nanosecond and sub-nanosecond laser pulses. In case of plasma investigations using nanosecond pulses, results of optical shadowgraphy, optical interferometry and X-ray pin-hole photography diagnostics are presented. However, for plasmas generated by sub-nanosecond laser pulse, only X-ray pinhole photography has been used. This was because; an ultra-short optical probe laser (few psec duration) was not available. However, in plasmas produced by the 5 nsec laser pulse, distinct features seen in the optical shadowgrams and interferograms are clearly reproduced in the X-ray pictures also. Hence, X-ray pinhole pictures could be reliably used to study the plasma ablation uniformity.

A fraction of the main laser beam was frequency upconverted to its second harmonic and used as an optical probe beam to record shadowgrams and interferograms of the expanding plasma. The optical diagnostic set ups have been described in detail in references [16] and [17] and the X-ray diagnostic are explained in [18]. The typical shadowgrams of aluminum and gold plasma at a laser intensity of 10^{13} W/cm^2 are shown in Fig. 6a and 6b respectively.

Corresponding interferogram are shown in Fig 7a. and 7b.

Ablating plasma X-ray pictures have been recorded using a X-ray pin-hole camera are shown in Fig. 8. The schematic set up of the pin-hole camera is shown in Fig. 8a. The X-ray pinhole picture for gold and aluminium are shown in Fig. 8(b) and (c) respectively.

The inset in Fig. 8a shows the digitized X-ray pinhole picture of plasma produced from a copper target using the sub-nanosecond laser pulse. These pictures have been recorded to show the distinct difference in the ablation

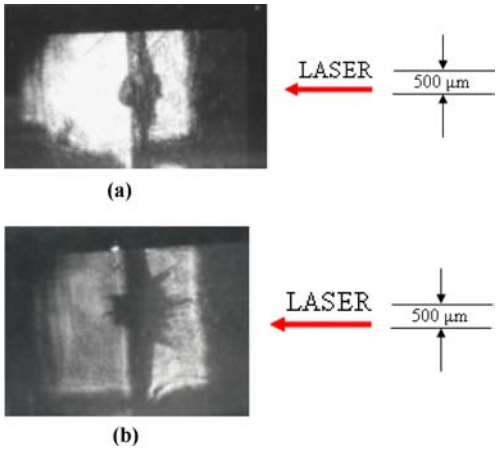

Figure 6 (a) Optical Shadowgram for Aluminum plasma; (b) Optical Shadowgram for Gold plasma.

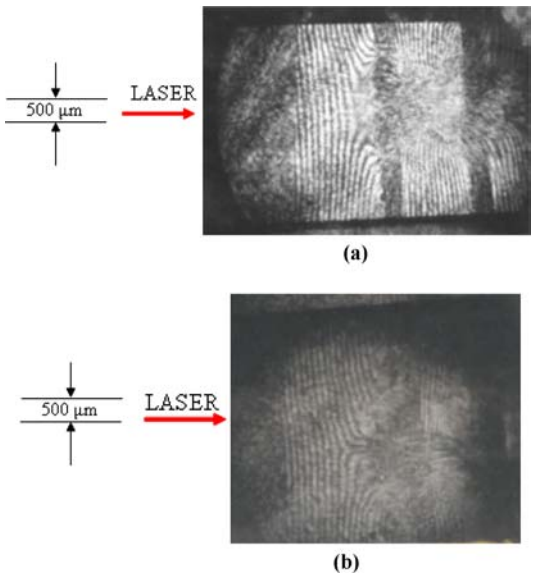

Figure 7 (a) Optical interferogram for Aluminum plasma; (b) Optical interferogram for Gold plasma.

profiles in the low Z aluminum and higher Z copper and gold plasma. These will be discussed in detail in the next section.

Ablating ion velocity has been measured using a Langmuir probe [20] placed inside the target chamber at a distance of 15 cm from the target and at 45^0 with respect to target normal as shown in Fig. 2. Langmuir probe signals for nanosecond and sub-nanosecond laser produced plasmas at identical laser intensity were recorded for materials of atomic numbers- 12(Mg), 13(Al), 22(Ti), 29(Cu) and 79(Au). Since the nature of signals for both laser pulse durations for a given target and at a given laser intensity were identical, only the signals obtained from the sub-nanosecond laser plasma are shown here. The typical ion signals from low Z and high Z targets obtained from the

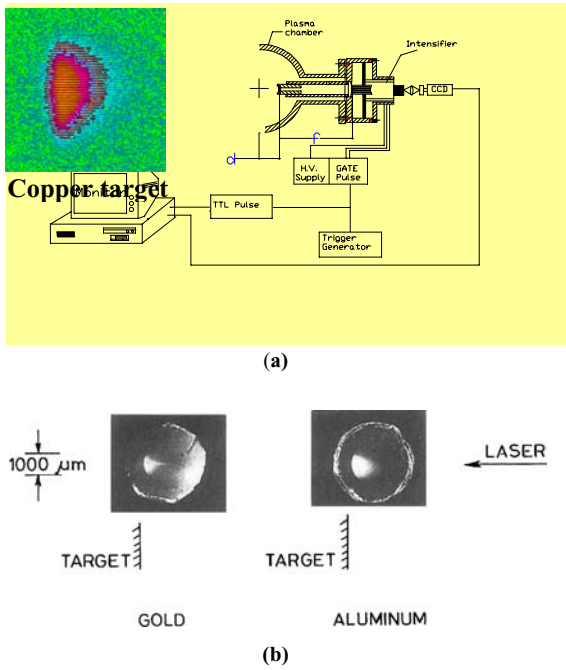

Figure 8 (a) Schematic set up of the X-ray pinhole camera. Copper plasma X-ray picture in the inset; (b) X-ray picture for gold plasma (c) X-ray picture for aluminum plasma.

Langmuir probe and displayed on a 500 MHz oscilloscope are shown in Fig. 9.

The time scale for the top four pictures (Mg, Al, Ti and Cu) is 0.1 μs/box and for the last (Au) it is 0.5 μs/box. The first signal indicated by an arrow in each picture is the X-ray signal from the plasma or what is known as the photo-peak, which is detected by the probe because of the emission of secondary electrons. Since X-ray emission from plasma occurs simultaneously with the laser pulse, the photo-peak is the time marker for the instant at which generation of plasma takes place or it is considered as the zero time. Time of flight of the ions is thus recorded with respect to the photo-peak and ion velocity can be calculated by knowing the distance of the probe from plasma. Peak of the ion signal designates the arrival time of the majority of ions.

3. 3. Results and discussions:

3.1. X-ray emission:

X-ray emission scaling with laser intensity for a 4 to 15 nsec [21, 22] laser pulse duration in copper targets has been earlier reported in our laboratory. Since we were interested in comparing the X-ray emission scaling for short laser pulses of 100 psec duration, copper was chosen as target material for this study. X-ray emission in arbitrary units from copper target irradiated by a sub-nanosecond laser pulse, detected by the two X-ray pin diodes has been plotted versus laser intensity in Fig. 5. The two linear

graphs indicate the signals from different parts of the X-ray emission spectrum from the plasma. The upper graph is for the 12μm thick Titanium filter foil which transmits X-rays from 2 KeV to almost 5 KeV as shown in Fig. 4a. On the other hand, the lower graph corresponds to the signal from the pin diode covered with a 5μm thick Nickel foil which transmits from 3 to 8.3 KeV. The Titanium foil thus transmits more on the softer side of the spectrum compared to the Nickel foil. The height of X-ray signals shown in Fig. 4b shows a higher signal in the softer part of the spectrum. In copper plasma, line radiation due to the L-shell emission is below 2 KeV and the K-shell emission is beyond 8 KeV. Therefore essentially, both the pin diodes are detecting the bremsstrahlung emission from the plasma. We have simulated the copper plasma at the laser intensity 5 X 10^{12} W/cm^2 and found the plasma temperature to be about 80 eV. The bremsstrahlung X-ray emission from 2 to 5 KeV has to be higher as compared to emission in the range 3 to 8 KeV. This is observed to be so in Fig. 5. Slope of the linear fit to both the graphs in Fig. 5 shows a value 2.02. X-ray emission intensity, I_x is thus observed to vary with laser intensity as $(I_L)^{2.02}$. The scaling exponent for 4 nsec laser plasmas was reported to be between 1.9 to 2.5 [21, 22] by other authors. It is thus observed that X-ray emission scaling exponent does not depend strongly upon the laser pulse duration.

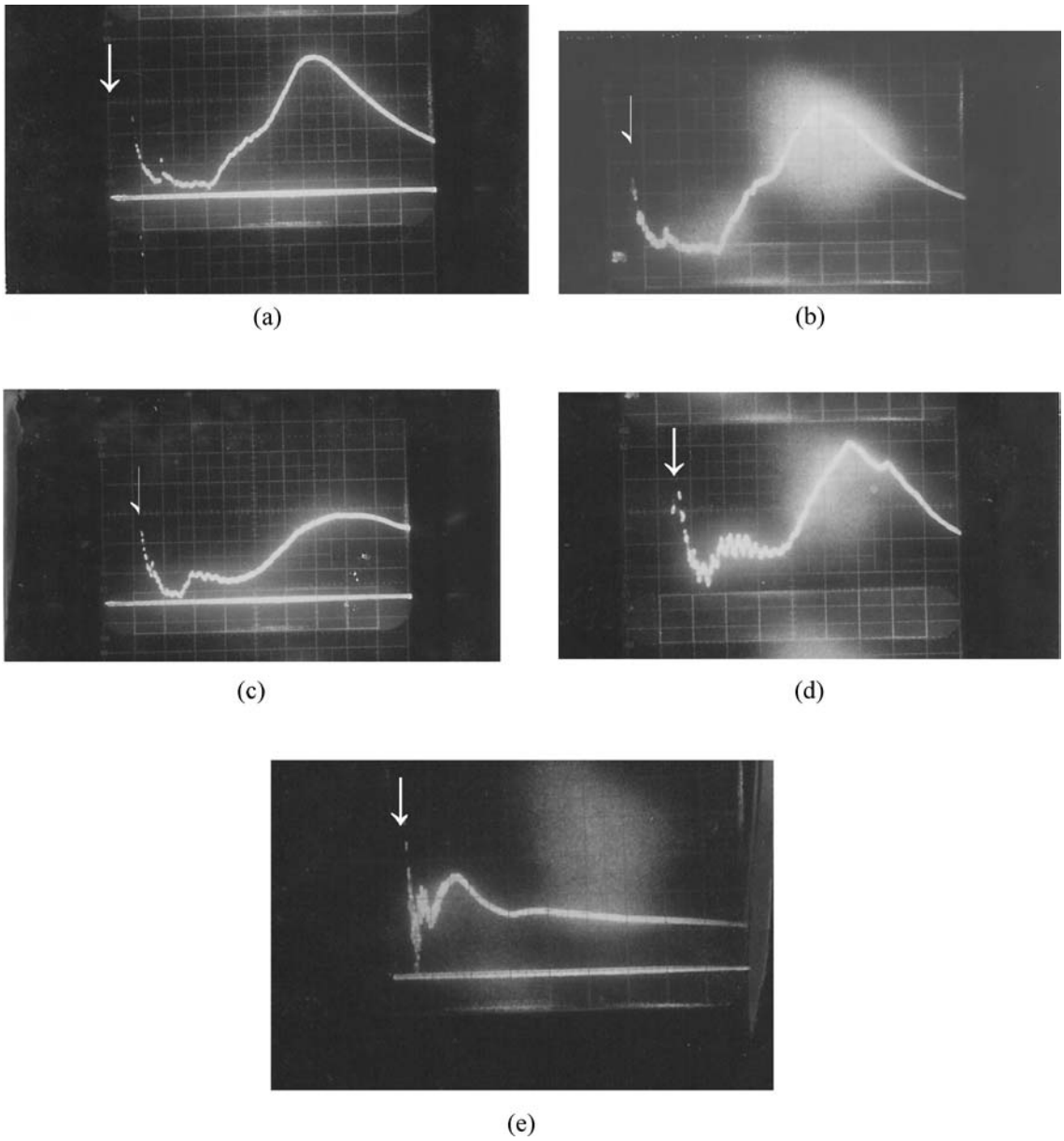

Figure 9 Ion signals from targets of varying atomic numbers. X-axis is time, Y-axis is ion current. Arrows show the position of the photopeak (a) Magnesium (b) Aluminum (c)Titanium (d) Copper (e) Gold

3.2. Ion emission:

The ion signals from plasma generated by the 100 psec laser pulse are shown in Fig. 9. The X-axis is time and vertical axis indicates the ion current. It is observed, that, for the lower atomic number targets, that is in Magnesium (Z = 12) and Aluminum (Z = 13) targets, there exists a single peak in the ion signal which corresponds to the majority of the ions. The ion expansion velocity corresponding to this peak (using time of flight) is 2.7×10^7 cms/sec for Magnesium and 2.4×10^7 cms/sec for Aluminum respectively. However, in Titanium (22), two peaks are clearly visible, indicating two groups of ions having different velocities. Whereas, majority of ions have a velocity 2×10^7 cms/sec (corresponding to the second slower peak), the velocity corresponding to the first peak is 7.5×10^7cms/sec, which corresponds to the fast ions. Multiple peaks are exhibited in copper and gold as well. In copper and gold, we can clearly observe three peaks. In copper, the last peak corresponds to the slowest ions. Ion expansion velocity corresponding to this peak is 2.2×10^7cms/sec, the middle peak corresponding to the set of faster ions have a velocity 2.9×10^7 cms/sec and the first peak corresponds to the fastest ions which have a velocity 10^8 cms/sec. Similarly, in gold, three bunches of ions with a velocity 0.93×10^7 cms/sec, 2.5×10^7 cms/sec and 10^8 cms/sec, and are seen. The optical shadowgrams, optical interferograms and X-ray pin hole pictures for Aluminum and gold are shown in Figs. 6, 7 and 8. All these pictures show the evolution of the ablating plasma at a given laser intensity and at a given instant of time. In all these pictures we can clearly observe that plasma ablation is uniform for aluminum. The ion probe signals also show a single peak indicating a uniform plasma expansion. However, in materials with a higher atomic number, for example in copper and gold, the shadowgrams, interferograms as well as the X-ray pinhole pictures show that there is a severe break up of the plasma. The ion signals also show a non-uniform plasma ablation in which there are groups of fast ions preceding the majority of ions.

Plasma jets or plasma break up has been studied extensively by several authors [23–25] and we also have studied and reported some of the results related to plasma jets [26, 27] in the past using nanosecond laser pulses to generate the plasma. In that work, we have presented an analytical model for the plasma jets which explains the various conditions in plasma necessary for the growth of this kind of instability. These jets have been ascribed due to radiation cooling instabilities when plasma from a high atomic number target with higher radiative losses expands in vacuum. In our earlier experimental work, we have shown some of the special features of these plasma jets, such as- increased plasma density and X-ray emission from the region of plasma jets. In the present experimental results we clearly observe an additional feature, that is, a striking correlation between appearance of fast ions in plasmas from high Z targets and the appearance of plasma jets in these targets. This is a direct evidence that ions in plasma jet travel with a higher velocity compared to background plasma. This to our knowledge is the first report on such an observation.

It is also of interest to note that plasma jets are formed not only in plasmas generated by laser pulses of several nanosecond duration, but, also in plasmas produced by 100 psec laser pulse. We observe that in case of nanosecond laser plasmas where the gradient scale lengths are long, length of the plasma jets are long as seen in Fig. 6b, 7b and 8b. In plasmas produced by short laser pulse of 100 secs, the length of plasma jets are small as seen in the digitized X-ray pin hole picture in Fig. 8a.

In the experimental results of Gabl *et al* [28] it has been shown that plasma jets move faster with respect to the background plasma. This was proved by them by measuring the length of plasma jet at different time using a framing camera. Correlation of fast ions and plasma jets in our experiments seems to corroborate the results of Gabl *et al*. The fast ions therefore, are emanating from these plasma jets. In such a situation, the ions within the plasma jets expand with a higher velocity as compared to the majority of ions from the background plasma. This would then result in the appearance of the fast peak in the ion signals. Optical interferogram of the expanding plasma from gold targets also shows increased plasma density within these jets, as indicated by the severe distortion of fringes in the region of the jets, as seen in Fig. 7b. The X-ray pinhole picture of gold plasma shown in Fig. 8b also clearly shows existence of plasma jets in gold plasma, having an enhanced emission of X-rays from this region compared to background plasma X-ray emission.

Latest reports by Kar *et al*. [29] using Vulcan Nd:Glass laser with 1psec duration and laser intensity of 10^{19}W/cm^2 also show development of jets in the ablating plasma. This shows that ablation of materials with higher atomic numbers irradiated by laser pulses of picosecond to several nanosecond duration and in a very wide range of intensity (10^{12} to 10^{19} W/cm^2) are always accompanied by fast moving plasma jets.

4. Conclusions

In these experiments we report that the X-ray scaling with laser intensity does not depend strongly upon the laser pulse duration. The scaling exponents for the 100 picosecond and nanoseconds laser pulse duration are observed to be almost in the same range. we have also observed that the laser produced plasmas from higher atomic number targets break up into small filamentary, jet like structures. These jets may be generated due to instabilities and lead to plasma break up. Plasma density and X-ray emission is higher in the region of these jets as compared to the background plasma. Appearance of plasma jets is always

accompanied by bunches of fast ions. It thus means that plasma jets expand at a higher velocity as compared to the background plasma. Jets are seen for plasmas generated by both nanoseconds and sub-nanosecond (100 psec) laser pulses. However, it is seen that in nanosecond plasmas, the jets are longer. This is understandable, since, any instability causing the formation of jets has a longer time to grow in a nanosecond laser plasma as compared in a sub-nanosecond laser plasma. Presently, it is not clear as to which physical mechanisms are responsible for the generation of the jets and bunches of fast ions of different velocities. This correlation of appearance of plasma jets in higher atomic number targets and generation of bunches of ions of higher velocity, to our knowledge, is the first observation. We are still trying to understand the mechanisms responsible for such enhanced acceleration of ions in plasma jets. Mechanisms responsible for jet formation in plasmas generated by- nanosecond, sub-nanosecond (100 psec) and few picosecond laser pulses may be different. However, this behavior of material ablation from laser irradiated high Z targets could have serious implications on laser based X-ray sources and X-ray lasers where laser-plasma ablation profiles have to be maintained uniform to a high degree. Several applications such as- thin film deposition by laser ablation, laser assisted ion implantation and X-ray driven Inertial Confinement Fusion scheme crucially depend upon the uniformity of expansion of the plasma. In the ICF scheme, plasma jets having fast ions emanating from the inner wall of the Hohlraum cavity could seriously impair the implosion of the target pellet placed within the Hohlraum cavity. Presence of plasma jets could also seriously affect the X-ray laser schemes.

Acknowledgments

The authors wish to acknowledge the support of B.S.Narayan, A.C. Shikalgar and Rajashree Vijayan for electronics support for the laser systems as well as the diagnostics.

References

1. M. KOENIG, in "Atoms, solids and plasmas in super-intense laser fields" (Kluwer Academic/Plenum, New York,2001) p. 327.; M. KOENIG *et al*., *Appl. Phys. Lett.* **72** (1998)1033.
2. R. CAUBLE, D. W. PHILLON, T. J. HOOVE, N. C. HOLMES, J. D. KILKENNY, R. W. LEE, *Phys. Rev. Lett.* **70** (1993) 2102.
3. J. C. GAUTHIER, in "Atoms, solids and Plasmas in super-intense laser fields"(Kluwer/Plenum Publishers, New York,2001) p. 223.
4. J. LINDL, *Physics of Plasmas.* **2**1995, 3933.
5. S. ELIEZER, in "Interaction of high-power lasers with plasmas" (Institute of Physics pub, Bristol,2002) p. 202.
6. A. LOVERIDGESMITH, A. ALLEN, J. BE LAK, T. BOEHLY, A. HAUER, B. HOLIAN, D. KALANTAR, G. KYRALA, R. W. LEE, P. LOMDAHL, M. MEYERS, D. PAISLEY, S. POLLAIN, B. REMINGTOND. C. SWIFT, S. WEBER and J. S. WARK, *Phys. Rev. Lett.* **86** (2001) 2349.
7. L. J. DHARESHWAR, P. A. NAIK, T. C. KAUSHIK and H. C. PANT, *Laser and Particle Beams.* **10** (1992) 201.
8. Idem.*High Pressure Research.* **10** (1992) 695.
9. L. J. DHARESHWAR and H. C. PANT, in Proceedings of the Fourteenth International Conference on Plasma Physics and Controlled Nuclear Fusion Research, Wurzburg, Germany, Sept,1992.
10. L. J. DHARESHWAR, N. GOPI, C. G. MURALI, B. S. NARAYAN, U. K. CHATTER-JEE, *Laser and Particle Beams.* **15** (1997) 297.
11. N. GOPI, R. C. BAPNA, B. S. NARAYAN, C. G. MURALI, L. J. DHARESHWAR and U. K. CHATTERJEE, in Advances in High pressure Science and Technology, edited byA. K. Singh (Tata McGraw-Hill, New Delhi,1994) p. 305.
12. L. J. DHARESHWAR and N. GOPI, in Proceedings of Third National Laser Symposium, Khargapur, India, Dec2003, edited by K. Bartwal(Allied Publishers, Kolkatta,2003) p. 295.
13. L. J. DHARESHWAR, N. GOPI, C. G. MURALI, R. C. BAPNA, B. S. NARAYAN, R. VIJAYAN and A. C. SHIKALGAR, "Development of a 10 GW (1J/100 psec) Nd: Glass Laser System" BARC Internal Report no: BARC/201/I/11, 2001.
14. L. J. DHARESHWAR, P. A. NAIK, H. C. PANT, *Journalof Physics* **27**(1986) 435.
15. C. G. MURALI, N. GOPI and L. J. DHARESHWAR, in Proceedings of Second National Laser Symposium, Indore, India, 2000 (Allied Publishers, Mumbai) p. 233.
16. L. J. DHARESHWAR, N. GOPI, H. ALI, S. K. GOEL and H. C. PANT, " Interferometric technique of measuring electronic density profiles in laser produced plasmas from solid targets" BARC Report no: BARC/I-726 (1982).
17. L. J. DHARESHWAR, P. A. NAIK, S. SHARMA and H. C. PANT, *Journal of Physics* **25** (1985) 63.
18. S. CHAURASIA, C. G. M. MURALI, L. J. DHARESHWAR, R. VIJAYAN and B. S. NARAYAN, presented in 19th National Symposium on Plasma, Jhansi, India, Dec 2004.
19. L. J. DHARESHWAR, N. GOPI, N. K. GUPTA and B. S. NARAYAN, Presented at National Laser Symposium, Indore, India, Dec 1999.
20. R. H. HUDDLESTONE and S. L. LEONARD, in "Plasma Diagnostic Techniques", 1965 (Academy Press, New York), Chapter 4.
21. R. SAUBREY *et al*., *Phys. Plasmas* **1**(1994) 1635.
22. Y. B. S. R. PRASAD, V. K. SANECHA, H. C. PANT and M. P. KAMAT, *Pramana, Journal of Physsics*, **56**(2000) 797.
23. O. WILLI and P. T. RUMSBY, *Optics Communication* , **37** (1981) 45.
24. G. THIELL, B. MEYER, *Laser and Particle Beams*, **3** (1985)51.
25. M. BORGHESI *et al*., Phys. Rev. Lett **81** (1998) 112.
26. L. J. DHARESHWAR, P. A. NAIK, P. D. NANDWANA and *H. C. PANT*, *J. Appl. Phys*, **61**(9) (1987) 4458.
27. L. J. DHARESHWAR, P. A. NAIK, S. SARKAR, M. KHAN, B. CHAKRABORTY, *Phys. Fluids*, **B4(6)** (1992) 1635.
28. E. F. GABL, B. H. FAILOR, C. J. ARMENTROUT, N. D. DELAMATER, W. B. FECHUER, G. E. BUSH, Z. M. KOENIG, D. RESS, L. SUTER, R. J. SCHROEDER, *Phys, Rev. Lett*, **63**(1989) 2737.
29. S. KAR, M. BORGHESI, L. ROMAGNANI, A. J. MACKINNON, P. K. PATEL, M. KEY, A. SCHIAVI, O. WILLI and A. MACCHI, in Central Laser Facility Annual Report no: RAL-TR-2004-025 (2003-2004) p. 24.

Received 30 March
and accepted 26 April 2005